General Physiology and Biophysics
Revised manuscript #1

Title: Antioxidative effects of diallyl trisulfide on hydrogen peroxide-induced cytotoxicity through regulation of nuclear factor-E2-related factor-mediated thioredoxin reductase 1 expression in C2C12 skeletal muscle myoblast cells

Running title: Antioxidative effects of diallyl trisulfide
Create date: 2016-09-05

Name	*Affiliations*
PhD Yung Hyun Choi	1. Department of Biochemistry, Anti-Aging Research Center , Dongeui University College of Korean Medicine , Busan, Korea, Republic Of
MS Ji Sook Kang	1. Anti-Aging Research Center and Blue-Bio Industry RIC, Dongeui University, Busan, South Korea
PhD Byung Woo Kim	1. Department of Life Science and Biotechnology, College of Natural Sciences & Human Ecology, Dongeui University, Busan, South Korea
PhD Gi Yiung Kim	1. Laboratory of Immunobiology, Department of Marine Life Sciences, Jeju National University, Jeju , South Korea

Corresponding author: PhD Yung Hyun Choi <choiyh@deu.ac.kr>

Abstract
Diallyl trisulfide (DATS) is one of the major constituents among the sulfur-containing compounds in garlic oil. Although DATS has strong radical scavenging and antioxidant activities, how DATS protects against oxidative stress is not fully understood. In this study, we analyzed the effects of DATS against hydrogen peroxide (H2O2)-induced oxidative stress in C2C12 myoblasts and to investigate the molecular mechanisms involved in this process. DATS preconditioning significantly attenuated H2O2-induced growth inhibition and DNA damage, as well as apoptosis in C2C12 cells by suppressing the generation of reactive oxygen species (ROS). Treatment with DATS alone effectively upregulated the expression of nuclear factor-erythroid 2-related factor 2 (Nrf2) and thioredoxin reductase 1 (TrxR1), which was associated with the increased phosphorylation of Nrf2. However, the protective effects of DATS against H2O2-induced growth reduction and ROS accumulation were significantly abolished by auranofin, an inhibitor of TrxR activity. Moreover, DATS-mediated phosphorylation of Nrf2 and induction of TrxR1 were markedly reduced by genetic silencing of Nrf2 using small interfering RNA. Esculetin treatment also induced the phosphorylation extracellular signal-regulating kinase (ERK), and analysis using specific inhibitors of cellular signaling pathways demonstrated that only ERK activation was involved in Nrf2 phosphorylation and TrxR1 induction. In addition, the potentials of DATS to protect against H2O2-induced apoptosis and growth inhibition were abrogated in C2C12 cells pretreated with an ERK specific inhibitor. The results demonstrate that DATS protects against oxidative stress-induced DNA damage and apoptosis in C2C12 cells in part through the activation of Nrf2-mediated TrxR1 induction via the ERK signaling pathway.

Keywords: DATS; oxidative stress; Nrf2; TrxR1; ERK

Response to reviews:
response to reviews file - download

Antioxidative effects of diallyl trisulfide on hydrogen peroxide-induced cytotoxicity through regulation of nuclear factor-E2-related factor-mediated thioredoxin reductase 1 expression in C2C12 skeletal muscle myoblast cells

Ji Sook Kang[1], Gi Yiung Kim[2], Byung Woo Kim[1,3], and Yung Hyun Choi[1,4,*]

[1]Anti-Aging Research Center and Blue-Bio Industry RIC, Dongeui University, 176 Eomgwangno Busanjin-gu, Busan 614-714, Republic of Korea

[2]Laboratory of Immunobiology, Department of Marine Life Sciences, Jeju National University, Jeju 690-756, Republic of Korea

[3]Department of Life Science and Biotechnology, College of Natural Sciences & Human Ecology, Dongeui University, Busan 614-714, Republic of Korea

[4]Department of Biochemistry, Dongeui University College of Korean Medicine, 52-57, Yangjeong-ro, Busanjin, Busan 614-052, Republic of Korea

Running Title: Antioxidative effects of diallyl trisulfide

Keywords: DATS, oxidative stress, Nrf2, TrxR1, ERK

Correspondence to:
Yung Hyun Choi
Department of Biochemistry, Dongeui University College of Korean Medicine, 52-57, Yangjeong-ro, Busanjin, Busan 614-052, Republic of Korea
E-mail: choiyh@deu.ac.kr

Abstract. Diallyl trisulfide (DATS) is one of the major constituents among the sulfur-containing compounds in garlic oil. Although DATS has strong radical scavenging and antioxidant activities, how DATS protects against oxidative stress is not fully understood. In this study, we analyzed the effects of DATS against hydrogen peroxide (H_2O_2)-induced oxidative stress in C2C12 myoblasts and to investigate the molecular mechanisms involved in this process. DATS preconditioning significantly attenuated H_2O_2-induced growth inhibition and DNA damage, as well as apoptosis in C2C12 cells by decreasing the generation of ROS. Treatment with DATS alone effectively upregulated the expression of nuclear factor-erythroid 2-related factor 2 (Nrf2) and thioredoxin reductase 1 (TrxR1), which was associated with the increased phosphorylation of Nrf2. However, the protective effects of DATS against H_2O_2-induced growth reduction and ROS accumulation were significantly abolished by auranofin, an inhibitor of TrxR activity. Moreover, DATS-mediated phosphorylation of Nrf2 and induction of TrxR1 were markedly reduced by genetic silencing of Nrf2 using small interfering RNA. Esculetin treatment also induced the phosphorylation extracellular signal-regulating kinase (ERK), and analysis using specific inhibitors of cellular signaling pathways demonstrated that only ERK activation was involved in Nrf2 phosphorylation and TrxR1 induction. In addition, the potentials of DATS to protect against H_2O_2-induced apoptosis and growth inhibition were abrogated in C2C12 cells pretreated with an ERK specific inhibitor. The results demonstrate that DATS protects against oxidative stress-induced DNA damage and apoptosis in C2C12 cells in part through the activation of Nrf2-mediated TrxR1 induction *via* the ERK signaling pathway.

Introduction

Oxidative stress reflects an imbalance between the systemic manifestation of reactive oxygen species (ROS) and a biological system's ability to readily detoxify the reactive intermediates or to repair the resulting damage all components of the cell, including proteins, lipids, and DNA (Lyakhovich and Graifer, 2015; Ermakov et al., 2013). Oxidative stress can cause disruptions in normal mechanisms of cellular signaling and is thought to be involved in the development of various diseases, such as cancer, neurodegenerative disease, and cardiovascular disease (Dai et al., 2014; Brieger et al., 2012). In contrast, antioxidant enzymes have been shown to have highly effective and sufficient for protecting cells against oxidative stress, and have some preventive or therapeutic effects against the symptoms of these diseases, particularly in those for which oxidative stress is the main cause (Mena et al., 2009). Therefore, therapeutic strategies should be focused on the reduction of free radical formation and scavenging of free radicals.

Most of the genes for encoding phase II detoxification or antioxidant enzymes are regulated via the redox-sensitive nuclear factor-E2-related factor (Nrf2) pathway (Silva-Palacios et al., 2016; Huang et al., 2015). Under unstimulated conditions, Nrf2 is kept in the cytosol bound to cytoskeleton Kelch-like ECH-associated protein 1 (Keap1), which acts as substrate adaptor for the Cul3-Rbx1 E3 ligase which ubiquitylates Nrf2 for proteasomal degradation (O'Connell et al., 2015; Jaramillo and Zhang, 2013). Dissociation of this complex is achieved by thiol modification of Keap1 preventing degradation and allowing newly synthesized Nrf2 to translocate into the nucleus where it binds to the antioxidant responsive element (ARE) in conjunction with other

transcription factors (Gan and Johnson, 2014; Jaramillo and Zhang, 2013). In the nucleus, Nrf2 associates with small Maf proteins, forming heterodimers that bind to ARE to activate the transcription of enzymes involved in the cellular antioxidant defense and in phase II detoxification, such as NAD(P)H:quinone oxidoreductase 1 (NQO1), thioredoxin (Trx) 1, Trx reductase (TrxR) 1, and heme oxygenase-1 (HO-1) (Cebula et al., 2015; Murakami and Motohashi, 2015; Stefanson and Bakovic, 2014). Recent observations demonstrated that the regulation of Nrf2-ARE mediated gene expressions requires the activation of several signal transduction pathways, including mitogen-activated protein kinases (MAPKs), such as extracellular signal-regulated kinase (ERK), c-Jun N-terminal kinase (JNK), p38 MAPK, phosphatidylinositol 3-kinase (PI3K)/protein kinase B (PKB, Akt), and nuclear factor kappa-B (NF-κB) (Jeong et al., 2006; Li et al., 2007; Hamdulay et al., 2010; Paine et al., 2010). They are important enzymes involved in the transduction of various signals from the cell surface to the nucleus associated with the modulation of ARE-driven gene expression *via* Nrf2 activation. Therefore, genes regulated by an ARE encode proteins that help to control cellular redox status and protect cells from oxidative damage.

Garlic (*Allium sativam* L.) is a plant commonly used for seasoning food in many different cultures, particularly in Asian countries, and an important component in the complementary and alternative medicine (Yun et al., 2014; Li et al., 2013). Recent data convincingly pointed out that garlic has a wide range of biological activities against a number of chronic diseases, including cardiovascular disorders, diabetes, infections, and other metabolic ills as well as cancer (Trio et al., 2014; Khatua et al., 2013; Padiya and Banerjee, 2013). Garlic is a particularly rich source of organosulfur compounds (OSCs), and diallyl monosulfide (DAS), diallyl disulfide (DADS), and diallyl trisulfide (DATS)

are the most abundant compounds in garlic oil (Lea, 1996; Amagase et al., 2001; Iciek et al., 2009). The antioxidant potential is in the order DATS > DADS > DAS (Liu et al., 2014; Jakubíková and Sedlák, 2006; Chen et al., 2004; Fukao et al., 2004), suggesting that the number of sulfur atoms plays a vital role in the biological activities of OSCs. Recently, Liang et al. (2015) suggested that DATS acts faster as an H_2S donor compared to DADS, which also supports these results.

Although several published reports have recently described the protective effects of DATS associated with Nrf2 signaling against oxidative stress (Xu et al., 2015; Kim et al., 2014; You et al., 2013; Tsai et al., 2013), the mechanism underlying its inductive effect remains largely unknown. This study was carried out to examine the ability of DATS to protect cells from hydrogen peroxide (H_2O_2)-induced cell damage and to elucidate the mechanism underlying these protective effects using a C2C12 murine skeletal-muscle cell line.

Materials and Methods

Reagents and antibodies

DATS (allyl trisulfide, Di-2-propenyl trisulfide) was purchased from LKT Laboratories (St Paul, MN, USA). Dulbecco's modified Eagle's medium (DMEM), fetal bovine serum (FBS) and other tissue culture reagents were obtained from WelGENE Inc. (Daegu, Republic of Korea). H_2O_2, 3-(4,5-dimethylthiazol-2-yl)-2,5-diphenyltetrazolium bromide (MTT), auranofin, N-acetyl-l-cysteine (NAC), 4',6-diamidino-2-phenylindole (DAPI), and propidium iodide (PI) were purchased from Sigma-Aldrich Chemical Co. (St. Louis, MO, USA). 2′,7′-dichlorofluorescein diacetate

(DCFDA) and annexin V-fluorescein isothiocyanate (FITC) apoptosis detection kit were purchased from Molecular Probes (Eugene, OR, USA) and R&D Systems Inc. (Minneapolis, MN, USA), respectively. Inhibitors of PI3K/Akt (LY294002) and MAPKs (SB203580, SP600125, and PD98058) were obtained from Calbiochem (San Diego, CA, USA). Primary antibodies were purchased from Santa Cruz Biotechnology (Santa Cruz, CA, USA) and Cell Signaling Technology (Danvers, MA, USA). Enhanced chemiluminescence (ECL) kit and horseradish peroxidase (HRP)-conjugated secondary antibodies were obtained from Amersham Life Science (Arlington Heights, IL, USA). All other chemicals not specifically cited here were purchased from Sigma-Aldrich Chemical Co.

Cell culture and DATS treatment

C2C12 cells obtained from American Type Culture Collection (Manassa, VA, USA) were maintained in DMEM supplemented with 10% fetal bovine serum (FBS) and 1% antibiotics (100 U/ml penicillin and 100 μg/ml streptomycin), and incubated at 37°C in a water-saturated atmosphere of 95% ambient air and 5% CO_2. DATS was dissolved in dimethyl sulfoxide (DMSO), and adjusted to the desired final concentrations using complete culture medium.

Cell viability assay and morphological imaging

For the cell viability study, cells were grown to 70% confluence and treated with DATS in the presence or absence with other agents(s). Control cells were supplemented with complete media containing 0.1% dimethylsulfoxide (DMSO) as the vehicle control. Following treatment, cell viability was determined by use of the MTT assay, which is

based on the conversion of MTT to MTT-formazan by mitochondrial enzymes. Optical density was measured at 540 nm with an enzyme-linked immunosorbent assay (ELISA) plate reader (Dynatech MR-7000; Dynatech Laboratories, Chantilly, VA, USA). The optical density of the formazan formed in control cells was used to represent 100% viability (Hong et al., 2016). Morphological changes of cells were monitored by obtaining photomicrographs under an inverted phase contrast microscope (Carl Zeiss, Oberkochen, Germany) with a digital camera.

Lactate dehydrogenase (LDH) release assay

The amount of LDH released from the cells in the supernatant was detected using an LDH assay kit (Sigma-Aldrich Chemical Co.) according to manufacturer's instructions. Briefly, at the end of the treatment period, culture medium was collected and transferred to new 96-well plates, then mixed with the 100 μl reaction solution provided in the kit for 30 min. The optical density was measured at 490 nm using an ELISA plate reader.

Comet assay (Single-cell gel electrophoresis assay)

A comet assay was performed to detect DNA migrating from single cells in the gel, following previously described method (Gunasekarana et al., 2015). Briefly, cells were exposed to H_2O_2 in the presence and absence of DATS. The cells were suspended in 1% low melting point agarose and aliquoted onto glass microscope slides. The slides were placed in single rows and electrophoresed at 30 V (1 V/cm) and 300 mAmp for 20 min to draw negatively charged DNA toward the anode. Finally, the slides were washed with 0.4 M Tris (pH 7.5) at 4°C and stained with 20 μg/ml PI. The slides were examined under a fluorescence microscope (Carl Zeiss) and the resulting images were analyzed.

169

170 *Protein extraction and Western blot analysis*

171 Cells were harvested, washed with phosphate-buffered saline (PBS) and lysed on ice for
172 30 min in lysis buffer (20 mM sucrose, 1 mM ethylenediaminetetra acetic acid, 20 μM
173 Tris-HCl, pH 7.2, 1 mM dithiothreitol, 10 mM KCl, 1.5 mM $MgCl_2$, and 5 μg/ml
174 aprotinin). Subsequently, an equal amount of protein for each sample was separated by
175 sodium dodecyl sulfate (SDS)-polyacrylamide gel electrophoresis and transferred to
176 PVDF membranes (Schleicher & Schuell, Keene, NH, USA). The membranes were
177 blocked with 5% skim milk and then incubated overnight at 4°C with desired primary
178 antibodies. The membranes were further incubated with corresponding HRP-conjugated
179 secondary antibodies for 2 h at room temperature. The proteins of interest were
180 visualized using an ECL detection system.

181

182 *Detection of nuclear morphological changes*

183 Detection of chromatin condensation and nuclear fragmentation in the nuclei of
184 apoptotic cells was performed by DAPI staining. The cells were harvested, washed with
185 PBS twice, and fixed with 3.7% paraformaldehyde in PBS for 10 min at 25°C. The
186 fixed cells were washed with PBS and stained with 1 mg/ml DAPI solution for 10 min.
187 The cells were washed twice with PBS and observed by fluorescence microscopy (Zhao
188 et al., 2014).

189

190 *Measurement of ROS generation*

191 To measure ROS levels, cells were washed twice with PBS and lysed with 1% Triton
192 X-100 in PBS for 10 min at 37°C and the cells then were stained with 10 μM DCFDA

for 20 min at room temperature in the dark. The green fluorescence of DCF was recorded at 515 nm (FL1) using a flow cytometer, and 10,000 events were counted per sample. The results were also expressed as the percentage increase relative to non-treated cells.

Flow cytometrydetection of apoptosis

The rate of apoptosis was determined using an annexin V-FITC apoptosis detection kit. After treatment with agents, the cells were stained with annexin V-FITC and PI in each sample in accordance with the manufacturer's instructions (Kwon et al., 2015). After 15 min incubation at room temperature in the dark, the degree of apoptosis was quantified as a percentage of the Annexin V-positive and PI-negative (Annexin V^+/PI^- cells) cells using a flow cytometer (Becton Dickinson, San Jose, CA, USA).

siRNA transfection

siRNA-mediated silencing of Nrf2 gene was performed using siRNA duplexes purchased from Santa Cruz Biotechnology according to the manufacturer's protocol. An unrelated siRNA with random nucleotides was used as the non-silencing control. The siRNA was transfected into cells according to the manufacturer's instruction using the Lipofectamine 2000 Transfection Reagent (Life Technologies, Carlsbad, CA, USA). For transfection, the cells were seeded in 6-well culture plates and incubated with 50 nM of control siRNA or Nrf2 siRNA in serum-free OPTI-MEM medium. After incubation for 6 h, the transfection medium was replaced with fresh media containing 10% FBS for 24 h before further manipulation described (Choi et al., 2016).

Statistical analysis

Unless specified otherwise, data are expressed as the mean ± standard deviation (SD) of at least three independent experiments. A one-way analysis of variance (SPSS version 12.0 software) followed by Scheffe's test was applied to determine the significance of differences between groups. A p value < 0.05 was considered significant.

Results

DATS inhibits H_2O_2-induced cytotoxicity

C2C12 cells were treated with 1.25 - 15 μM DATS for 6 h to determine the effect of DATS on C2C12 cell viability using a MTT assay. The treatments did not result in any cytotoxic effect up to the concentration of 5 μM, and cell viability dose-dependently decreased at concentrations higher than 7.5 μM (Fig. 1A). DATS concentrations less than 5 μM) were selected for the subsequent examination of the protective effect of DATS on H_2O_2-induced cytotoxicity. Treatment with 1 mM H_2O_2 significantly reduced cell viability about 40%; this H_2O_2-induced reduction of cell viability was concentration-dependently protected by pretreatment with DATS (Fig. 1B). We also determined C2C12 cell damage by LDH assay. As shown in Fig. 1C, the H_2O_2-treated cells exhibited an induced LDH release as compared with the control, whereas pretreatment of cells with DATS markedly attenuated LDH release in a concentration-dependent manner. In addition, H_2O_2 stimulation significantly induced morphological changes including extensive cytosolic vacuolization and the presence of irregular cell membrane buds, which were effectively attenuated by DATS pretreatment (Fig. 1C). These results indicate that DATS may protect C2C12 cells from H_2O_2-induced damage.

241

242 *DATS protects against H_2O_2-induced DNA damage*

243 We next examined the effects of DATS on H_2O_2-mediated DNA damage in C2C12 cells.
244 A comet assay showed that exposure to H_2O_2 led to loss of membrane integrity, with
245 fragmented DNA resolved outside the cell as comet-like structures; this adverse effect
246 was markedly inhibited by DATS pretreatment (Fig. 2A). In addition, immunoblotting
247 results indicated that treatment of C2C12 cells with H_2O_2 upregulated the level of the
248 phosphorylated histone variant H2AX at serine 139 (p-γH2AX), a sensitive marker of
249 DNA double-strand breaks (Rogakou et al., 1988) (Fig. 2C). Pretreatment with DATS
250 significantly reduced H_2O_2-induced p-γH2AX expression.

251

252 *DATS protects against H_2O_2-induced apoptosis*

253 To evaluate the potential effect of DATS on H_2O_2-induced C2C12 cell apoptosis, we
254 examined apoptotic features by measuring the chromatin condensation of the nuclei and
255 poly(ADP ribose) polymerase (PARP) cleavage. DAPI staining revealed increased
256 nuclei with chromatin condensation and the formation of apoptotic bodies, which are
257 characteristic morphological changes of apoptosis, in cells cultured with H_2O_2.
258 However, the control and DATS alone treated groups showed few apoptotic cells, and
259 pretreatment of the cells with DATS significantly abrogated H_2O_2-induced apoptotic
260 characteristics (Fig. 2C). Immunoblotting results also indicated that there was a marked
261 increase in the level of cleaved PARP, a protein marker of apoptosis, in H_2O_2-treated
262 cells compared with the control; treatment with DATS significantly decreased this
263 cleavage (Fig. 2D).

264

DATS reduces H_2O_2-induced ROS generation

Intracellular ROS generation was monitored by flow cytometry to investigate whether DATS could prevent H_2O_2-induced ROS generation. Significantly increased ROS level was detected after 1 mM H_2O_2 treatment unlike in untreated cells; however, this increase was significantly reduced in the presence of 5 μM DATS (Fig. 3A). As a positive control, the ROS scavenger NAC (5 mM) also markedly attenuated H_2O_2-induced ROS generation and DATS itself did not contribute to the ROS generation, indicating that DATS scavenged H_2O_2-induced ROS accumulation. Flow cytometry analysis revealed increased number of annexin-positive cells in the H_2O_2-treated C2C12 cells compared to that in the control group. In contrast, the treatment of cells with DATS prior to H_2O_2 exposure protected the C2C12 cells against apoptosis (Fig. 3B).

Cytoprotective effect of DATS against oxidative stress is mediated through TrxR1 induction

To determine whether that the protective effects of DATS against H_2O_2-induced oxidative stress and apoptosis result from the induction of antioxidant genes, such as TrxR1, NQO-1, and HO-1, and their transcription factor Nrf2 and Keap1, a repressor of Nrf2, Western blot analyses were performed. DATS enhanced TrxR1 expression, but not Keap1, NQO-1 and HO-1, in time- and concentration-dependent manners; the enhanced expression was associated with increased expression and phosphorylation of Nrf2 (Fig. 4). Therefore, C2C12 cells were pre-treated with auranofin, which is widely used as an inhibitor of TrxR activity (Roder and Thomson, 2015; Liu et al., 2000), in the presence or absence of DATS and then exposed to H_2O_2, to identify whether the TrxR is involved in the protective effect of DATS. Auranofin significantly abrogated

289 the protective effect of DATS on H_2O_2-induced reduction of cell viability and
290 production of ROS (Fig. 5).
291
292 *DATS upregulates TrxR1 expression via Nrf2 activation*
293 To clarify the role of Nrf2 in TrxR1 upregulation in C2C12 cells, we developed an Nrf2
294 gene knockdown model using siRNA transfection. Compared to the control siRNA-
295 transfected cells, silencing Nrf2 through a specific siRNA eliminated the DATS -
296 induced expression of Nrf2 as well as its phosphorylation and TrxR1 induction (Fig.
297 6A). Moreover, the siNrf2 transfection abrogated the protective effects of DATS against
298 H_2O_2-induced growth reduction unlike in the control siRNA-transfected cells (Fig. 6B).
299
300 *DATS enhances Nrf2 phosphorylation by ERK*
301 To investigate whether Nrf2 phosphorylation by DATS in C2C12 cells might be
302 affected by activation of signaling pathways, such as PI3K/Akt and MAPKs as
303 upstream signaling mediators, we observed the phospho-forms of components of
304 PI3K/Akt and MAPKs. Although the total protein levels of ERK did not show notable
305 changes, DATS markedly increased the phosphorylation of ERK within 30 min of
306 treatment, while PI3K, Akt, JNK, and p38 MAPK remained unchanged in their
307 phosphorylation levels (Fig. 7A). The dependence of the induction and phosphorylation
308 of Nrf2 challenged with DATS upon the activation of either ERK was proven using a
309 specific inhibitor of ERK, PD98059. C2C12 cells were pretreated with 50 μM PD98059
310 for 1 h and then treated with esculetin for 6 h. PD98059 treatment effectively reduced
311 the DATS-induced induction and phosphorylation of Nrf2, with a resulting drop in the
312 induction of TrxR1 (Fig. 6C). However, treatment with other specific pharmacological

313 inhibitors of PI3K/Akt (LY294002), JNK (SP600125), and p38 MAPK (SB203580) did
314 not affect the expression of Nrf2 and TrxR1. In addition, co-pretreatment with PD98059
315 and DATS prior to the H_2O_2 exposure was able to remarkably abrogate the protective
316 effects of DATS against H_2O_2-induced apoptosis as well as growth reduction (Fig. 8).
317
318 **Discussion**
319
320 In the current study, DATS showed intracellular ROS scavenging activities and
321 provided cytoprotection against oxidative stress in C2C12 cells (Figs. 1 and 3A). DATS
322 antagonized H_2O_2-induced DNA damage and apoptosis accompanied with a significant
323 decrease of ROS generation (Figs. 2 and 3). These data support the view that the
324 protective effects of DATS contribute to its role in the ROS scavenging effect and the
325 antioxidant defense activity against H_2O_2 treatment in C2C12 cells.
326 Accumulating evidence indicates that Nrf2 is a critical regulator in the orchestration
327 of cellular antioxidant defenses and maintenance of redox homeostasis by mediating the
328 induction of a variety of antioxidant defense enzymes. Nrf2 has been implicated as a
329 therapeutic target for the prevention against oxidative stress-induced DNA damage and
330 apoptosis (Huang et al., 2015; Gan and Johnson, 2014). In addition, TrxR is a
331 nicotinamide adenine dinucleotide phosphate (NADPH)-dependent seleno cysteine-
332 containing flavoenzyme that catalyzes the reduction of oxidized Trx and other small
333 molecular oxidants (Mustacich and Powis, 2000; Arner, 2009). Therefore, the Trx
334 system, a thiol-dependent electron donor system comprising Trx, TrxR, and NADPH, is
335 critical in maintaining cellular redox homeostasis by counteracting the effects of ROS
336 and regulating redox-related signaling cascades (Nguyen et al., 2006; Arner and

337 Holmgren, 2000). The Trx system also has key roles in DNA synthesis and activation of
338 transcription factors that regulate cell growth (Holmgren and Lu, 2010; Kondo et al.,
339 2006). The present results demonstrate that DATS treatment leads to an increase in the
340 level of Nrf2 phosphorylation as well as the expression of Nrf2, and the expression of
341 its downstream antioxidant enzyme TrxR1, but not NQO1 and HO-1, in time- and
342 concentration-dependent manners (Fig. 4). To confirm that the protective effects of
343 DATS were due to Trx signaling, auranofin, an inhibitor of TrxR activity (Roder and
344 Thomson, 2015; Liu et al., 2000), was used. Our data indicate that induction of TrxR1
345 expression might be required to suppress H_2O_2-induced ROS generation and that the
346 anti-oxidative effects of DATS may occur through Trx signaling pathway (Fig. 5).
347 To further determine whether up-regulation of TrxR1 by DATS treatment is caused
348 by Nrf2 pathway, we transfected cells with Nrf2 siRNA followed by treatment with
349 DATS. Transfection with Nrf2 siRNA markedly attenuated DATS-induced TrxR1
350 expression compared to control along with the inhibition of Nrf2 phosphorylation (Fig.
351 6A), demonstrating that DATS could induce TrxR1 expression by activating Nrf2
352 signaling. In parallel with these observations, silencing Nrf2 reversed the protective
353 effects of DATS against H_2O_2-induced reduction of C2C12 cell viability (Fig. 6BC).
354 Therefore, we conclude that DATS treatment has a protective effect against H_2O_2-
355 mediated oxidative stress in C2C12 cells by activating the Nrf2-mediated TrxR1
356 signaling pathway.
357 Because several cellular signaling pathways including PI3K/Akt and MAPKs
358 represent important regulatory pathways for Nrf2 phosphorylation and nuclear
359 translocation associated with inducible expression of antioxidant enzymes (Kweon et al.
360 2006; Surh et al. 2008), the effects of DATS on PI3K/Akt and MAPKs cascades were

investigated to further identify the signaling pathways affected by DATS that enhance Nrf2 phosphorylation and TrxR1 expression. Immunoblotting results indicated that phosphorylation of ERK was observed at 30 min after DATS treatment and increased for up to 120 min, while PI3K, Akt, JNK, and p38 MAPK kinases were not affected (Fig. 7A). Therefore, we next examined the effects of specific inhibitors of PI3K/Akt and three MAPKs on the phosphorylation of Nrf2 as well as the increased levels of TrxR1. DATS-induced phosphorylation of Nrf2 and TrxR1 expression was markedly suppressed by PD98059, a specific inhibitor of ERK (Fig. 7B). However, other inhibitors did not dramatically affect Nrf2 phosphorylation and TrxR1 expression, implicating ERK as having the major role in Nrf2 phosphorylation in the induction of downstream TrxR1 expression in DATS-treated C2C12 cells. Importantly, blockage of ERK activation with PD98059 drastically attenuated the protective effects of DATS against H_2O_2-induced apoptosis and inhibition of the growth in C2C12 cells (Fig. 8). Taken together, these findings support the hypothesis that the ERK signaling pathway is involved in DATS-mediated activation of Nrf2 and upregulation of TrxR1. Thus, regulation of the Nrf2-mediated TrxR1 pathway can reduce H_2O_2-induced oxidative damage in C2C12 cells.

In summary, our results demonstrate that DATS protects C2C12 cells against oxidative stress-induced DNA damage and apoptosis through scavenging of ROS. Elevated activation of ERK signaling appears to be responsible for the activation of Nrf2 and its subsequent induction of TrxR1 expression. Although further research and clinical trials are needed to elucidate the molecular mechanisms detected herein, we suggest that DATS is able to reduce oxidative stress and ameliorate oxidative stress-related diseases.

Conflict of Interest

The author has no conflict of interest to declare.

Acknowledgements

This research was supported by Basic Science Research Program through the National Research Foundation of Korea (NRF) grant funded by the Korea government (2015R1A2A2A01004633) and the Blue-Bio Industry Regional Innovation Center (RIC08-06-07) at Dongeui University as a RIC program under Ministry of Trade, Industry & Energy and Busan city.

References

Amagase H., Petesch B. L., Matsuura H., Kasuga S., Itakura Y. (2001): Intake of garlic and its bioactive components. J. Nutr. **131**, 955S-9562S.

Arner E. S. (2009): Focus on mammalian thioredoxin reductases-important seleno-proteins with versatile functions. Biochim. Biophys. Acta. **1790**, 495-526.

Arnér E. S., Holmgren A. (2000): Physiological functions of thioredoxin and thioredoxin reductase. Eur. J. Biochem. **267**, 6102-6109.

Brieger K., Schiavone S., Miller F. J. Jr, Krause K. H. (2012): Reactive oxygen species: from health to disease. Swiss Med. Wkly. **142**, w13659.

Cebula M., Schmidt E. E., Arnér E. S. (2015): TrxR1 as a potent regulator of the Nrf2-Keap1 response system. Antioxid. Redox. Signal. **23**, 823-853.

Chen C., Pung D., Leong V., Hebbar V., Shen G., Nair S., Li W., Kong A. N. (2004): Induction of detoxifying enzymes by garlic organosulfur compounds through transcription factor Nrf2: effect of chemical structure and stress signals. Free Radic. Biol. Med. **37**, 1578-1590.

Choi E. O., Jeong J. W., Park C., Hong S. H., Kim G. Y., Hwang H. J., Cho E. J., Choi Y. H. (2016): Baicalein protects C6 glial cells against hydrogen peroxide-induced oxidative stress and apoptosis through regulation of the Nrf2 signaling pathway. Int. J. Mol. Med. **37**, 798-806.

Dai D. F., Chiao Y. A., Marcinek D. J., Szeto H. H., Rabinovitch P. S. (2014); Mitochondrial oxidative stress in aging and healthspan. Longev. Healthspan **3**, 6.

420 Ermakov A. V., Konkova M. S., Kostyuk S. V., Izevskaya V. L., Baranova A., Veiko N.
421 N. (2013): Oxidized extracellular DNA as a stress signal in human cells. Oxid. Med.
422 Cell. Longev. **2013**, 649747.
423 Fukao T., Hosono T., Misawa S., Seki T., Ariga T. (2004): The effects of allyl sulfides
424 on the induction of phase II detoxification enzymes and liver injury by carbon
425 tetrachloride. Food Chem. Toxicol. **42**, 743-739.
426 Gan L., Johnson J. A. (2014): Oxidative damage and the Nrf2-ARE pathway in
427 neurodegenerative diseases. Biochim. Biophys. Acta. **1842**, 1208-1218.
428 Gunasekarana V., Raj G. V., Chand P. (2015): A comprehensive review on clinical
429 applications of comet assay. J. Clin. Diagn. Res. **9**, GE01-5.
430 Hamdulay S. S., Wang B., Birdsey G. M., Ali F., Dumont O., Evans P. C., Haskard D.
431 O., Wheeler-Jones C. P., Mason J. C. (2010): Celecoxib activates PI-3K/Akt and
432 mitochondrial redox signaling to enhance heme oxygenase-1-mediated anti-
433 inflammatory activity in vascular endothelium. Free Radic. Biol. Med. **48**, 1013-1023.
434 Holmgren A., Lu J. (2010): Thioredoxin and thioredoxin reductase: current research
435 with special reference to human disease. Biochem. Biophys. Res. Commun. **396**, 120-
436 124.
437 Hong S. H., Sim M. J., Kim Y. C. (2016): Melanogenesis-promoting effects of
438 *Rhynchosia nulubilis* and *Rhynchosia volubilis* ethanol extracts in melana cells.
439 Toxicol. Res. **32**, 141-147.
440 Huang Y., Li W., Su Z. Y., Kong A. N. (2015): The complexity of the Nrf2 pathway:
441 beyond the antioxidant response. J. Nutr. Biochem. **26**, 1401-1413.
442 Iciek M., Kwiecień I., Włodek L. (2009): Biological properties of garlic and garlic-
443 derived organosulfur compounds. Environ. Mol. Mutagen. **50**, 247-265.

444 Jakubíková J., Sedlák J. (2006): Garlic-derived organosulfides induce cytotoxicity,
445 apoptosis, cell cycle arrest and oxidative stress in human colon carcinoma cell lines.
446 Neoplasma **53**, 191-199.
447 Jaramillo M. C., Zhang D. D. (2013): The emerging role of the Nrf2-Keap1 signaling
448 pathway in cancer. Genes Dev. **27**, 2179-2191.
449 Jeong W. S., Jun M., Kong A. N. (2006): Nrf2: a potential molecular target for cancer
450 chemoprevention by natural compounds. Antioxid. Redox. Signal. **8**, 99-106.
451 Khatua T. N., Adela R., Banerjee S. K. (2013): Garlic and cardioprotection: insights
452 into the molecular mechanisms. Can. J. Physiol. Pharmacol. **91**, 448-458.
453 Kim S., Lee H. G., Park S. A., Kundu J. K., Keum Y. S., Cha Y. N., Na H. K., Surh Y. J.
454 (2014): Keap1 cysteine 288 as a potential target for diallyl trisulfide-induced Nrf2
455 activation. PLoS One **9**, e85984.
456 Kondo N., Nakamura H., Masutani H., Yodoi J. (2006): Redox regulation of human
457 thioredoxin network. Antioxid. Redox. Signal. **8**, 1881-1890.
458 Kweon M. H., Adhami V. M., Lee J. S., Mukhtar H. (2006): Constitutive
459 overexpression of Nrf2-dependent heme oxygenase-1 in A549 cells contributes to
460 resistance to apoptosis induced by epigallocatechin 3-gallate. J. Biol. Chem. **281**,
461 33761-33772.
462 Kwon T., Rho J. K., Lee J. C., Park Y. H., Shin H. J., Cho S., Kang Y. K., Kim B. Y.,
463 Yoon D. Y, Yu D. Y. (2015): An important role for peroxiredoxin II in survival of
464 A549 lung cancer cells resistant to gefitinib. Exp. Mol. Med. **47**, e165.
465 Lea M. A. (1996): Organosulfur compounds and cancer. Adv. Exp. Med. Biol. **401**,
466 147-154.

Li J., Calkins M. J., Johnson D. A., Johnson J. A. (2007): Role of Nrf2-dependent ARE-driven antioxidant pathway in neuroprotection. Methods Mol. Biol. **399**, 67-78.

Li L., Sun T., Tian J., Yang K., Yi K., Zhang P. (2013): Garlic in clinical practice: an evidence-based overview. Crit. Rev. Food Sci. Nutr. 53, 670-681.

Liang D., Wu H., Wong M. W., Huang D. (2015): Diallyl trisulfide is a fast H_2S donor, but diallyl disulfide is a slow one: The reaction pathways and intermediates of glutathione with polysulfides. Org. Lett. 17, 4196-4199.

Liu J., Akahoshi T., Namai R., Matsui T., Kondo H. (2000): Effect of auranofin, an antirheumatic drug, on neutrophil apoptosis. Inflammation Res. **49**, 445-451.

Liu L. L., Yan L., Chen Y. H., Zeng G. H., Zhou Y., Chen H. P., Peng W. J., He M., Huang Q. R. (2014): A role for diallyl trisulfide in mitochondrial antioxidative stress contributes to its protective effects against vascular endothelial impairment. Eur. J. Pharmacol. **725**, 23-31.

Lyakhovich A., Graifer D. (2015): Mitochondria-mediated oxidative stress: Old target for new drugs. Curr. Med. Chem. **22**, 3040-3053.

Mena S., Ortega A., Estrela J. M. (2009): Oxidative stress in environmental-induced carcinogenesis. Mutat. Res. **674**, 36-44.

Murakami S., Motohashi H. (2015): Roles of Nrf2 in cell proliferation and differentiation. Free Radic. Biol. Med. **88**, 168-178.

Mustacich D., Powis G. (2000): Thioredoxin reductase. Biochem. J. **346**, 1-8.

Nguyen P., Awwad R.T., Smart D.D., Spitz D.R., Gius D. (2006): Thioredoxin reductases a novel molecular target for cancer therapy. Cancer Lett. **236**, 164-174.

O'Connell M. A., Hayes J. D. (2015): The Keap1/Nrf2 pathway in health and disease: from the bench to the clinic. Biochem. Soc. Trans. **43**, 687-689.

491 Padiya R., Banerjee S. K. (2013): Garlic as an anti-diabetic agent: recent progress and
492 patent reviews. Recent Pat. Food Nutr. Agric. **5**, 105-127.
493 Paine A., Eiz-Vesper B., Blasczyk R., Immenschuh S. (2010): Signaling to heme
494 oxygenase-1 and its anti-inflammatory therapeutic potential. Biochem. Pharmacol. **80**,
495 1895-1903.
496 Roder C., Thomson M.J. (2015): Auranofin: repurposing an old drug for a golden new
497 age. Drugs R. D. **15**, 13-20.
498 Rogakou E. P., Pilch D. R., Orr A. H., Ivanova V. S., Bonner W. M. (1998): DNA
499 double-stranded breaks induce histone H2AX phosphorylation on serine 139. J. Biol.
500 Chem. **273**, 5858-5868.
501 Silva-Palacios A., Königsberg M., Zazueta C. (2016): Nrf2 signaling and redox
502 homeostasis in the aging heart: A potential target to prevent cardiovascular diseases?
503 Ageing Res. Rev. **26**, 81-95.
504 Stefanson A. L., Bakovic M. (2014): Dietary regulation of Keap1/Nrf2/ARE pathway:
505 focus on plant-derived compounds and trace minerals. Nutrients **6**, 3777-3801.
506 Surh Y. J., Kundu J. K., Na H. K. (2008): Nrf2 as a master redox switch in turning on
507 the cellular signaling involved in the induction of cytoprotective genes by some
508 chemopreventive phytochemicals. Planta Med. **74**, 1526-1539.
509 Trio P. Z., You S., He X., He J., Sakao K., Hou D. X. (2014): Chemopreventive
510 functions and molecular mechanisms of garlic organosulfur compounds. Food Funct.
511 **5**, 833-844.
512 Tsai C. Y., Wang C. C., Lai T. Y., Tsu H. N., Wang C. H., Liang H. Y., Kuo W. W.
513 (2013): Antioxidant effects of diallyl trisulfide on high glucose-induced apoptosis are

514 mediated by the PI3K/Akt-dependent activation of Nrf2 in cardiomyocytes. Int. J.
515 Cardiol. 168, 1286-1297.
516 Xu X. H., Li G. L., Wang B. A., Qin Y., Bai S. R., Rong J., Deng T., Li Q. (2015):
517 Diallyl trisufide protects against oxygen glucose deprivation -induced apoptosis by
518 scavenging free radicals via the PI3K/Akt -mediated Nrf2/HO-1 signaling pathway in
519 B35 neural cells. Brain Res. **1614**, 38-50.
520 You S., Nakanishi E., Kuwata H., Chen J., Nakasone Y., He X., He J., Liu X., Zhang S.,
521 Zhang B., Hou D. X. (2013): Inhibitory effects and molecular mechanisms of garlic
522 organosulfur compounds on the production of inflammatory mediators. Mol. Nutr.
523 Food Res. **57**, 2049-2060.
524 Yun H. M., Ban J. O., Park K. R., Lee C. K., Jeong H. S., Han S. B., Hong J. T. (2014);
525 Potential therapeutic effects of functionally active compounds isolated from garlic.
526 Pharmacol. Ther. **142**, 183-195.
527 Zhao X., Sun P., Qian Y., Suo H. (2014): *D. candidum* has *in vitro* anticancer effects in
528 HCT-116 cancer cells and exerts in vivo anti-metastatic effects in mice. Nutr. Res.
529 Pract. **8**, 487-493.
530

Figure legends

Figure 1. DATS inhibits H_2O_2-induced cytotoxicity in C2C12 cells. Cells were treated with various concentrations of DATS for 6 h (A) or pretreated with the indicated concentrations of DATS for 1 h and then incubated with and without 1 mM H_2O_2 for 6 h (B). Cell viability was assessed using an MTT reduction assay. (C) The cytotoxicity was also measured by the LDH assay. The results represent the mean ± SD obtained in three independent experiments (*p<0.05 compared with control group; $^{\#}p$<0.05 compared with H_2O_2-treated group). (D) Cellular morphological changes were monitored in photomicrographs obtained using inverted phase contrast microscopy (x200).

Figure 2. Inhibition of H_2O_2-induced DNA damage and apoptosis by DATS in C2C12 cells. Cells were pretreated with 5 μM DATS for 1 h and then incubated with and without 1 mM H_2O_2 for 6 h. (A) To detect cellular DNA damage, the comet assay was performed and representative pictures of the comets were taken using fluorescence microscopy (x200 original magnification). (C) The cells were fixed and stained with DAPI. The stained nuclei were observed using fluorescent microscopy (x400 original magnification). (B and D) The cells were lysed and equal amounts of cell lysate (50 μg) were separated by SDS-PAGE and transferred to nitrocellulose membranes. The membranes were probed with specific antibodies against p-γH2AX, γH2AX, PARP, and actin (the latter as an internal control) and the proteins were visualized by ECL.

Figure 3. Inhibition of H_2O_2-induced ROS generation and apoptosis by DATS in C2C12 cells. Cells were pretreated with 5 μM DATS for 1 h and then incubated with or without 1 mM H_2O_2 for 6 h. (A) To monitor ROS production, the cells were incubated at 37°C in the dark for 20 min with new culture medium containing 10 μM DCFDA. ROS accumulation was measured using flow cytometry. (B) To quantify the degree of apoptosis, the cells were stained with annexin-V-FITC and PI for flow cytometry analysis. The results are the mean ± SD obtained in three independent experiments (*p<0.05 compared with the control group; $^{\#}p$<p0.05 compared with the H_2O_2-treated group).

Figure 4. Effects of DATS on the expression of Nrf2, TrxR1, NQO1, and HO-1 in C2C12 cells. Cells were incubated with 5 μM DATS for the indicated periods (A) or incubated for 6 h with the indicated concentrations of DATS (B). Cellular proteins were separated by SDS-PAGE and transferred to nitrocellulose membranes. The membranes were probed with the indicated antibodies. Proteins were visualized using ECL. Actin was used as an internal control.

Figure 5. Effects of TrxR inhibition on DATS-mediated attenuation of growth inhibition and ROS formation by H_2O_2 in C2C12 cells. Cells were pretreated for 1 h with 5 μM DATS and then treated for 6 h with or without 1 mM H_2O_2 in the absence or presence of 1 μM auranofin. Cell viability (A) and ROS generation (B) were estimated. The results are the mean ± SD values obtained in three independent experiments (*p<0.05 compared with control group; $^{\#}p$<0.05 compared with H_2O_2-treated group; $^{\$}p$<0.05 compared with H_2O_2 and DATS-treated group).

Figure 6. Nrf2-mediated induction of TrxR1 expression by DATS in C2C12 cells. Cells were transfected with control (Con siRNA, as a negative control for RNA interference) and Nrf2 siRNA. After 24 h, the cells were treated with 5 μM DATS for 6 h (A) in the presence or absence with 1 mM H_2O_2 (B). (A) Cellular proteins were separated by SDS-PAGE and transferred to nitrocellulose membranes. The membranes were probed with antibodies against Nrf2, p-Nrf2 and TrxR1. Proteins were visualized using ECL. Actin was used as an internal control. (B) Cell viability was assessed using a MTT reduction assay. The results are the mean ± SD values obtained in three independent experiments (*p<0.05 compared with control group; $^{\#}p$<0.05 compared with H_2O_2-treated group; $^{\$}p$<0.05 compared with H_2O_2 and Nrf2 siRNA-treated group).

Figure 7. Involvement of ERK signaling pathway on the induction of Nrf2 and TrxR1 by DATS in C2C12 cells. Cells were treated with 5 μM DATS for the indicated times (A) or pre-treated for 1 h with and without the indicated inhibitors (LY294002, a specific inhibitor of PI3K; PD98059, a specific ERK inhibitor; SB203580, a specific p38 MAPK inhibitor; SP600125, a specific JNK inhibitor), and then treated with 5 μM DATS for an additional 6 h (B). The cells were lysed, and then equal amounts of cell lysates were separated by SDS-PAGE and transferred to nitrocellulose membranes. The membranes were probed with the indicated antibodies, and the proteins were visualized using ECL. Actin was used as an internal control.

603 Figure 8. Effects of ERK inhibition on DATS-mediated attenuation of apoptosis and
604 growth inhibition by H_2O_2 in C2C12 cells. Cells were pretreated for 1 h with 5 μM
605 DATS and were subsequently treated for 6 h with or without 1 mM H_2O_2 in the
606 absence or presence of 50 μM PD98059. Apoptosis rate (A) and cell viability (B)
607 were estimated. The results are expressed as the mean ± SD values obtained in
608 three independent experiments (*p<0.05 compared with the control group;
609 $^{\#}p$<p0.05 compared with the H_2O_2-treated group; $^{\$}p$<p0.05 compared with the H_2O_2
610 and DATS treated group).

Fig. 1 Download full resolution image

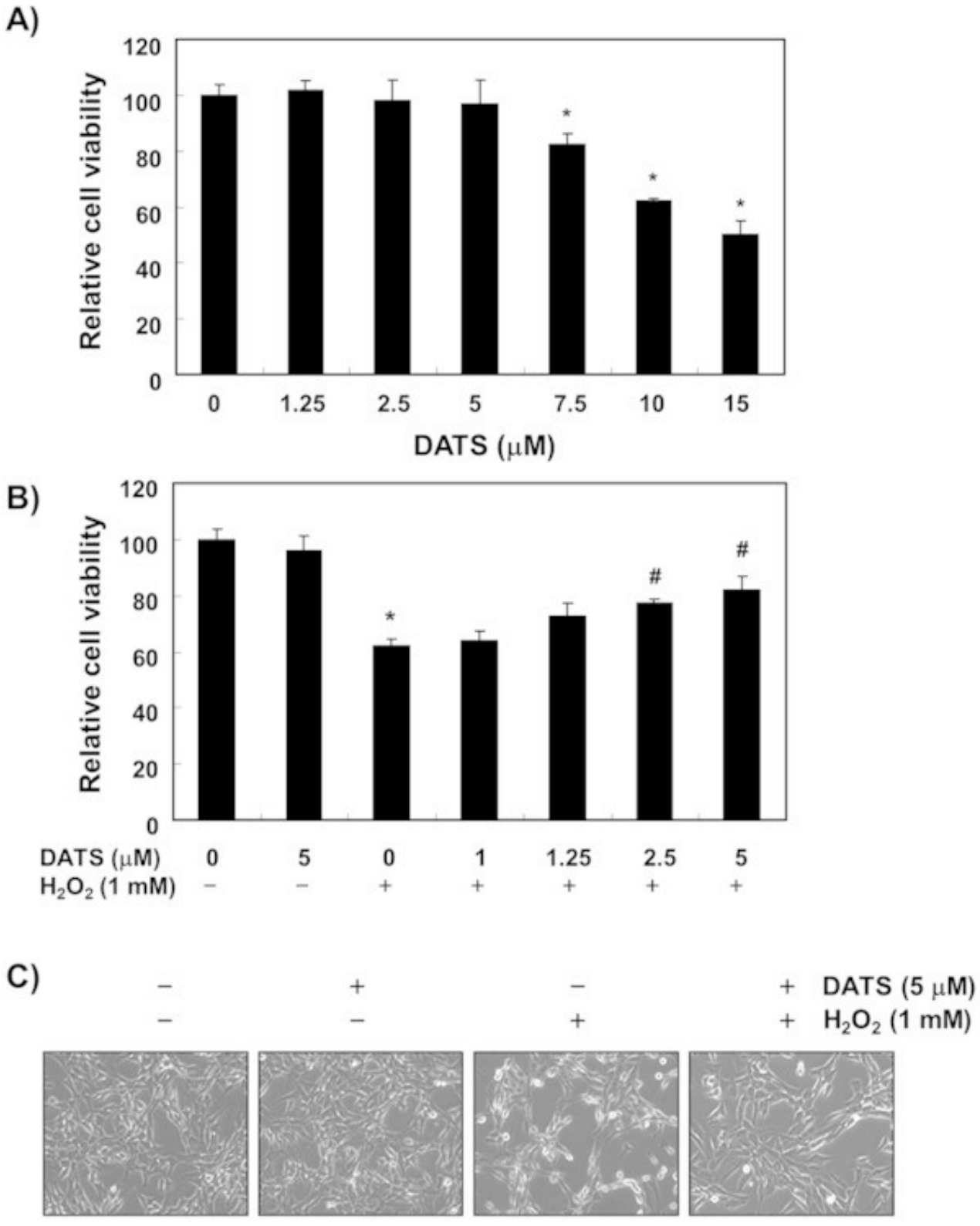

Fig. 2 Download full resolution image

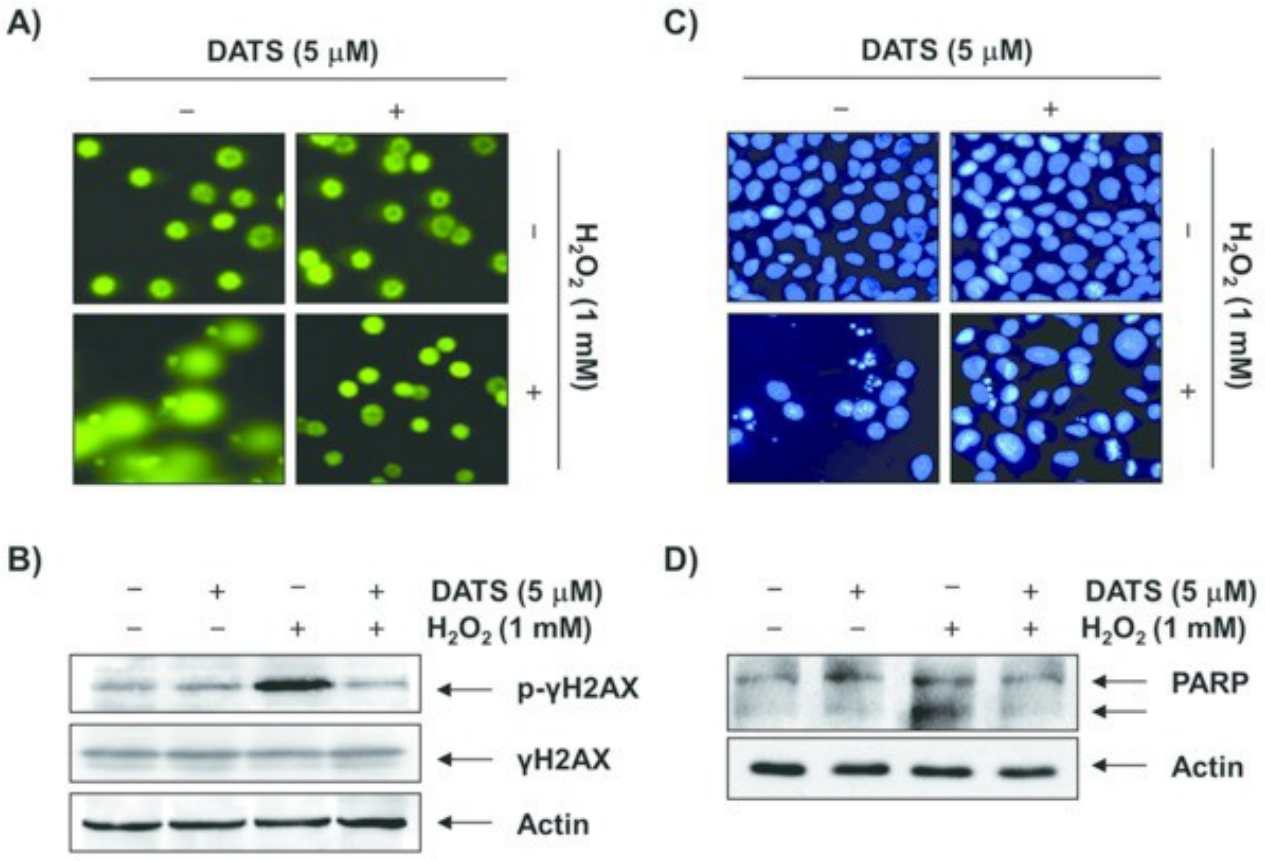

Fig. 3 Download full resolution image

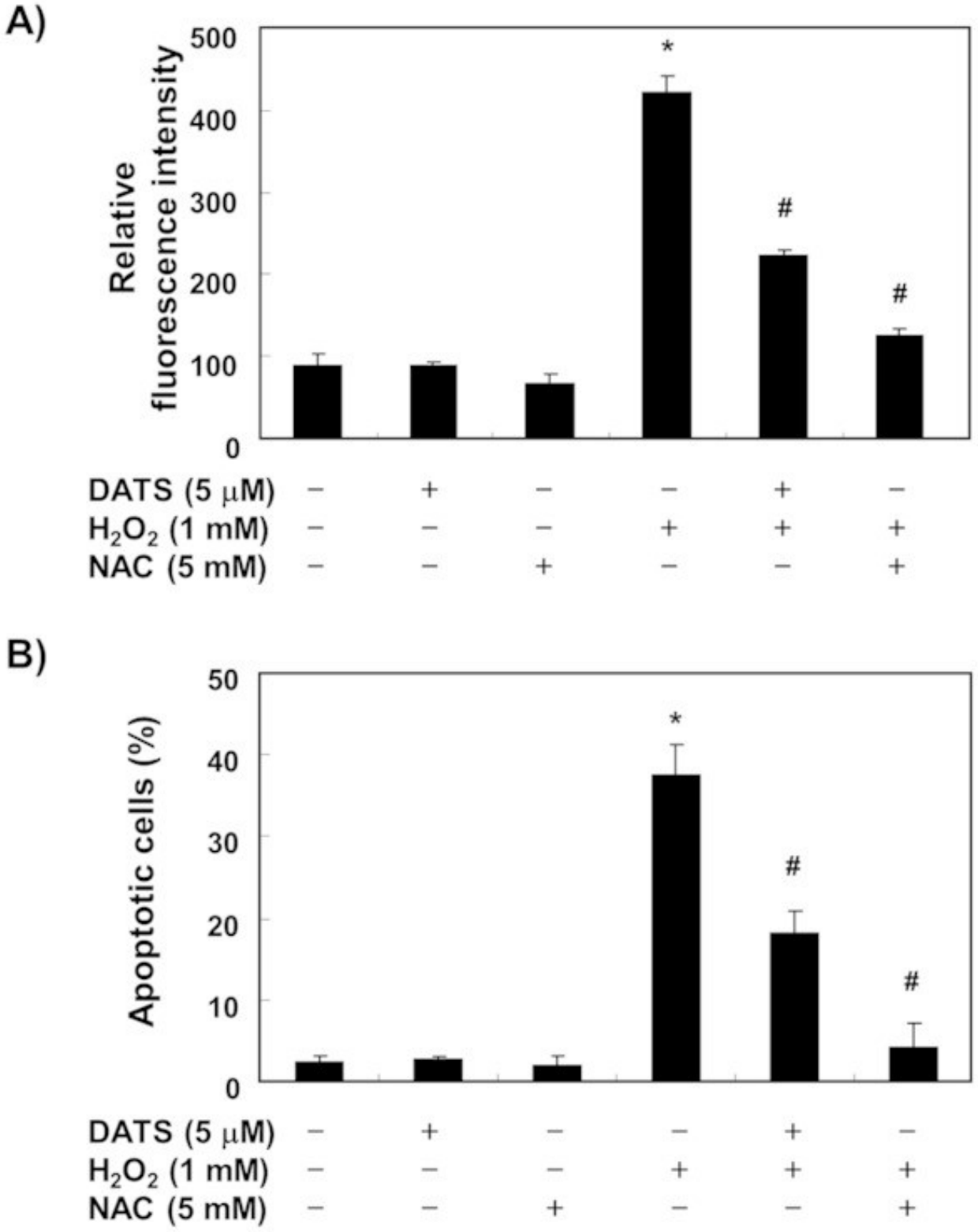

Fig. 4 Download full resolution image

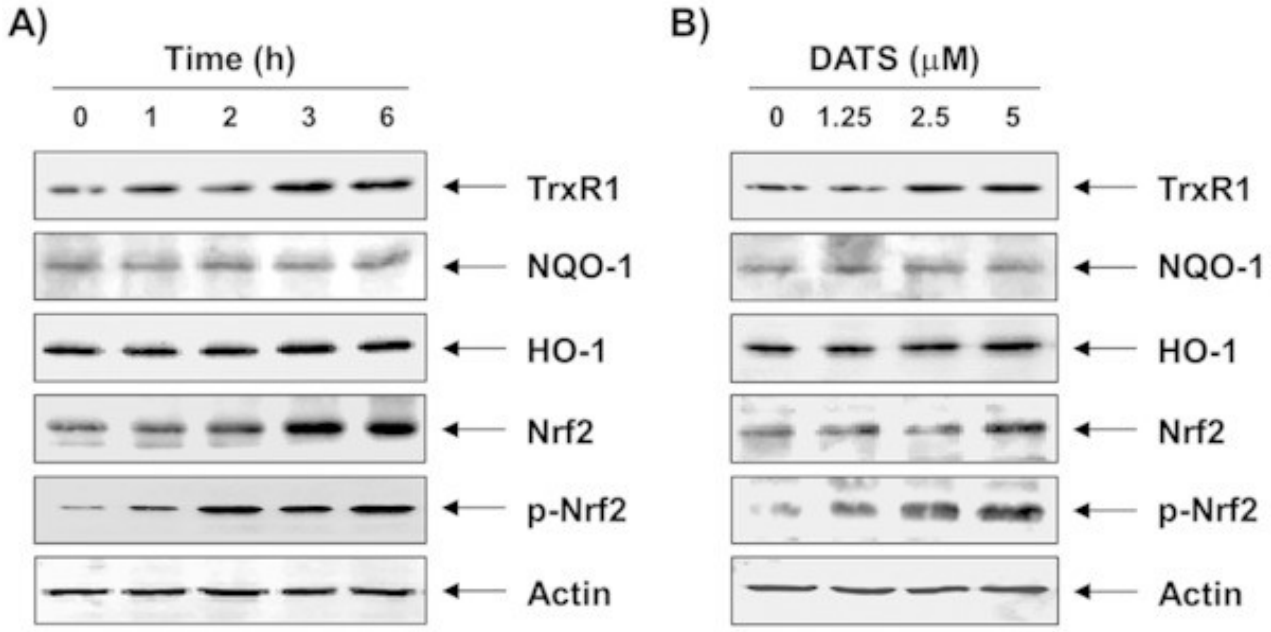

Fig. 5 Download full resolution image

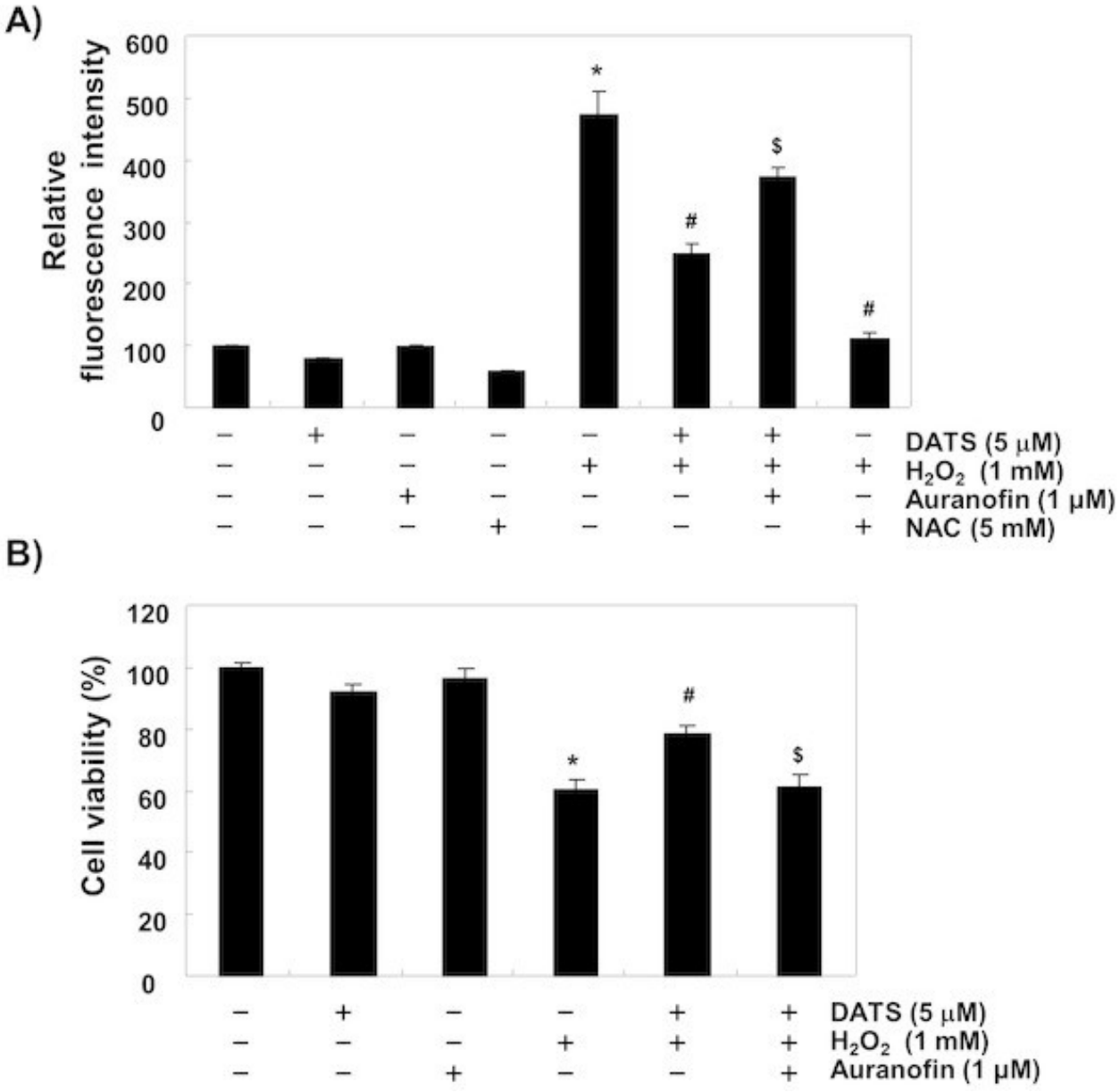

Fig. 6 Download full resolution image

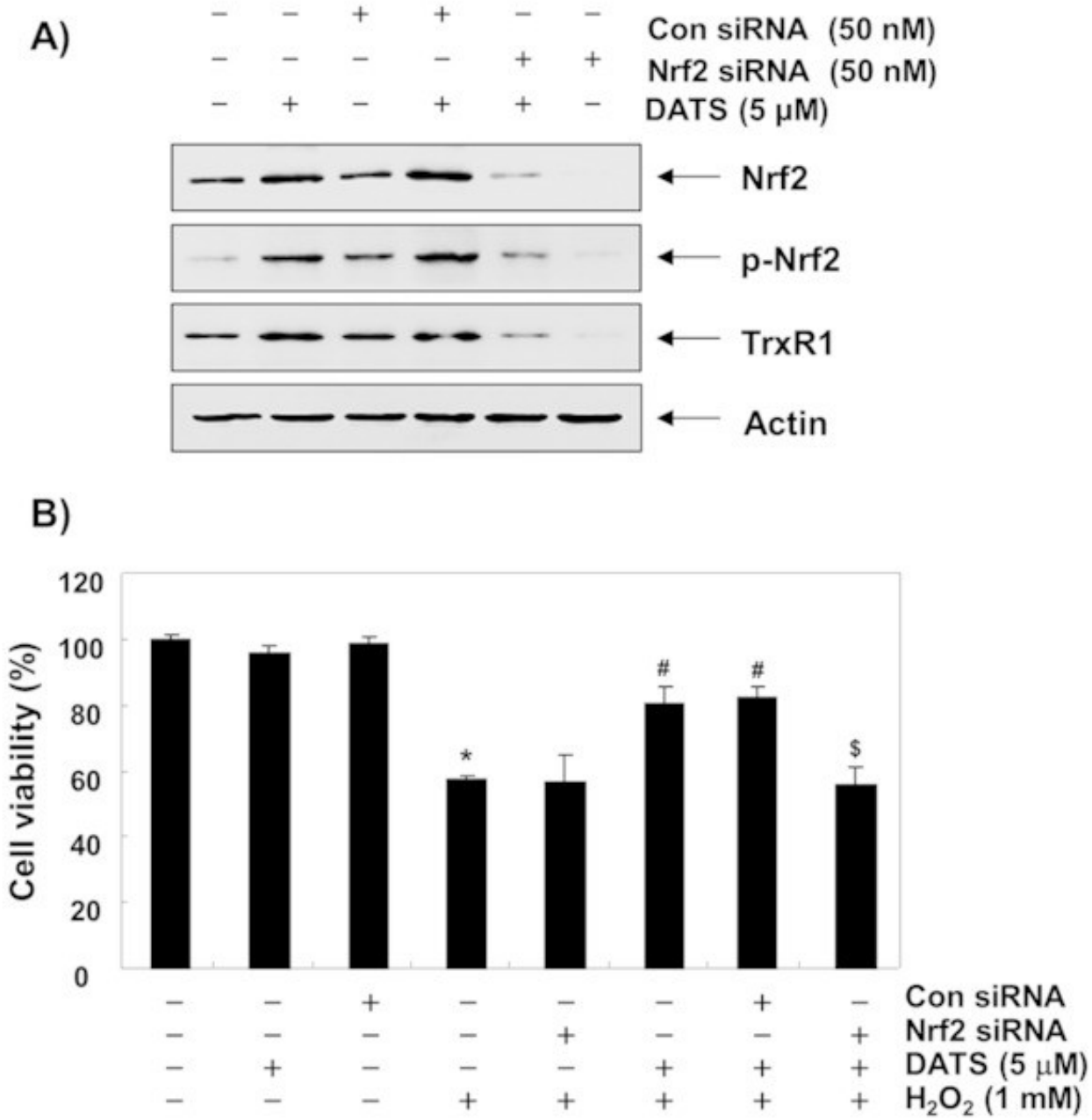

Fig. 7 Download full resolution image

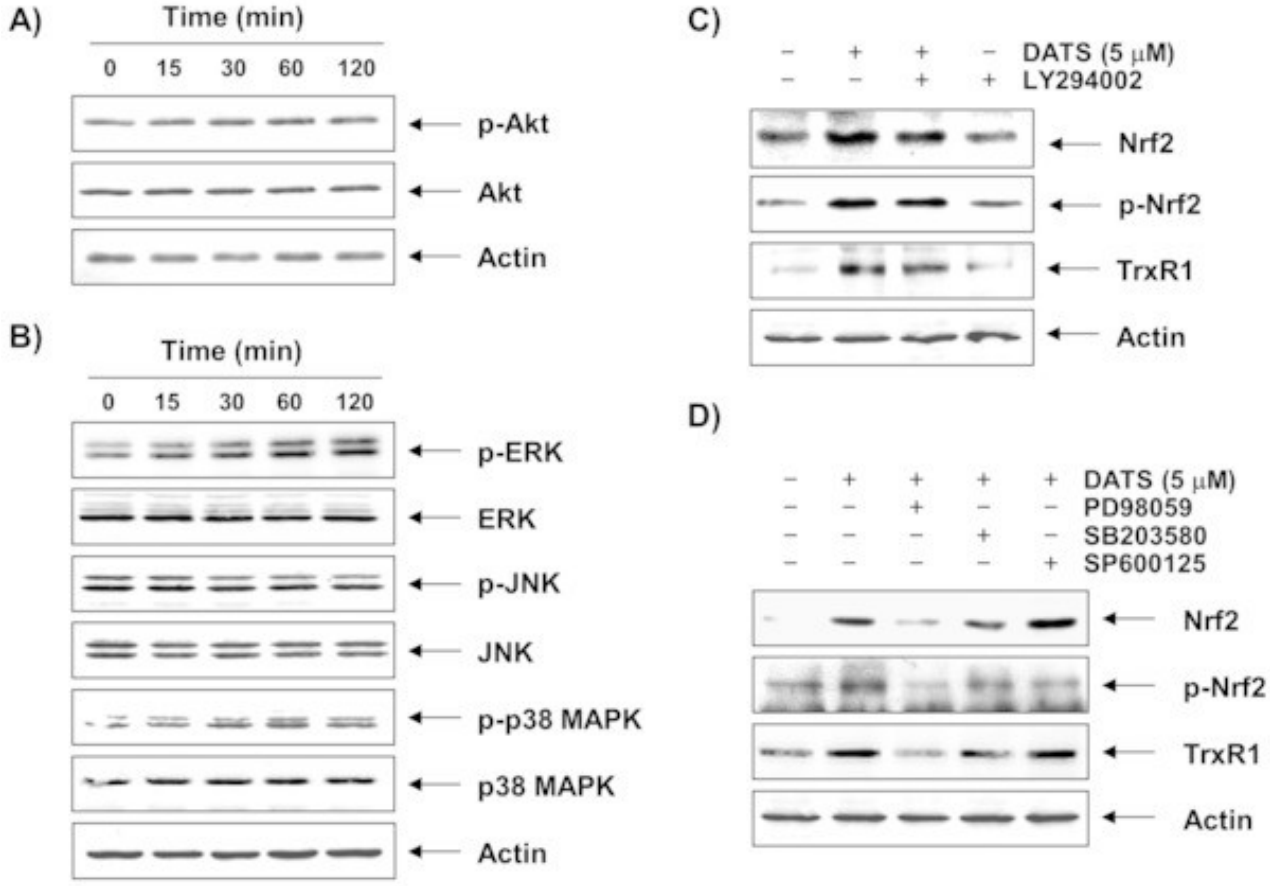

Fig. 8 Download full resolution image